



Resonant beam vibration: A wave evolution analysis

X.Q. Wang*, R.M.C. So, K.T. Chan

Department of Mechanical Engineering, The Hong Kong Polytechnic University, Hung Hom, Kowloon, Hong Kong

Received 7 January 2004; received in revised form 22 April 2005; accepted 23 June 2005

Available online 24 August 2005

Abstract

In an attempt to verify the concept of wave-mode duality and to understand the wave-train closure principle in resonant beam vibration, an elastically supported beam subjected to a swept sinusoidal force is investigated through a simulation of wave evolution from initial to final steady-state response. Wave evolution is simulated in the superposition and the degenerate states according to the nature of wave reflection at the boundaries of the beam. From the results, resonance condition is established, and the natural frequencies and mode shapes are calculated. Using a simply supported beam and a cantilever beam as examples, the concept of wave-mode duality at resonance is verified. An examination of the wave-train closure principle shows that, although the frequency equations obtained by using the principle are identical to those derived from the wave evolution results, the principle does not describe the realistic process of the formulation of vibration modes in general. The waves described in the wave-train closure principle are not physical but “virtual” waves that represent final steady-state waves, which can only be asymptotically approached in reality. The principle can be used as a convenient technique to obtain vibration modes from the point of view of wave propagation.

© 2005 Elsevier Ltd. All rights reserved.

1. Introduction

A vibrating system can be studied in terms of either vibration modes or propagating waves. The former approach (referred to as the mode approach thereafter) has been a standard one in vibration analysis, normally implemented by the method of modal expansion for simple structures

*Corresponding author. Tel.: +852 2766 5111; fax: +852 2365 4703.

E-mail address: mmxqwang@polyu.edu.hk (X.Q. Wang).

and by the finite element method for complex structures. In the mode approach, free vibration is treated as an eigenvalue problem mathematically, and forced vibration is analyzed as a linear combination of the eigenfunctions (modes). The latter approach (referred to as the wave approach thereafter), represented by the method of statistical energy analysis [1,2], is particularly successful in the field of vibro-acoustics and high-frequency vibration analysis, where the mode approach is not practical because the density of modes in the frequency domain becomes very large and the influence of structure uncertainty is significant. The statistical energy analysis technique has also been applied to treat vibration problems for various built-up structures [3–8].

In principle, the results obtained by the mode approach and the wave approach are consistent. This is termed the wave-mode duality and is considered to be a fundamental concept for a comprehensive understanding of sound and vibration problems [9] to be obtained. While the mode approach is convenient and efficient to use, the wave approach may provide more physical insight into the vibration phenomenon being investigated. For example, vibration modes of a beam were shown to be superposed standing waves through a wave mechanics approach [10], and the physics of the “second spectrum” of beam vibration was elaborated.

In recent years, hybrid methods were developed to combine the advantages of the mode and the wave approaches, giving rise to a unified approach for vibration analysis in a wider frequency range. Such an approach is either based on an extension of the statistical energy analysis technique [11–14], or on the modification of the finite element method, termed as the spectral element method [15–18] or the continuous element method [19]. On the other hand, relatively little attention has been paid to a theoretical justification of the wave-mode duality in various dynamic systems.

For a system carrying one type of wave, the wave-mode duality was discussed by Langley [20]. When the system is one-dimensional, free vibration analysis showed that vibration modes of such a system are equivalent to the addition of traveling waves. At off-resonance, it was shown by forced vibration analysis that the superposition of traveling waves could be converted to modal expansion results using the Mittag-Leffler expansion. When the system is two-dimensional, however, the results of the wave approach were found to be non-unique. This leaves a question for further investigation. Chen [21] showed that axial vibration of a rod can be expressed as the addition of either infinite numbers of standing waves or infinite numbers of traveling waves. This can be regarded as an example of the wave-mode duality.

A one-dimensional system may carry multiple types of wave with different wave number at the same frequency. One example is the beam. Chan et al. [10] showed that a beam accommodates two types of flexural waves, known as the k_a - and k_b -waves, respectively. In general, vibration modes can only be formulated by superposing the flexural waves, i.e., superposed standing waves. The wave-mode duality in such a system also has not been addressed.

On the other hand, the wave-train closure principle given by Cremer and Heckl [22] could be regarded as an expression of wave-mode duality for free vibration analysis, in the sense that it describes the process of the formulation of a standing wave (vibration mode). The principle states that, in order to formulate a standing wave, a propagating wave must return to its starting point after completing one complete circuit of the system with the same amplitude and phase, i.e., it closes on itself. From the superposed-standing-wave point of view, this principle was applied to Timoshenko beams by Wang and So [23]. A more complex behavior of wave reflection at the boundaries of the beam was demonstrated. It was found that one type of incident wave would produce two types of reflected waves in general. In certain cases, however, one wave leads to only

one reflected wave of the same type. These two wave-reflection behaviors were called the superposition and the degenerate states of wave reflection, respectively, which lead to different types of standing waves (vibration modes).

The objective of the present study is to verify the concept of wave-mode duality in resonant beam vibration and to elaborate on a physical understanding of the wave-train closure principle by simulating wave evolution in a beam from initial response due to external excitation to final steady-state response. A uniform beam with general elastic end supports subjected to a point excitation at an arbitrary location along the beam is considered. The excitation force is a continuous sinusoidal one with its frequency varying within the whole spectrum, and may thus be regarded as a swept sinusoidal excitation. Since wave reflection at the boundary can be in the superposition or the degenerate state, the process of wave evolution for these two cases is studied accordingly. The steady-state response of the beam is obtained by adding initial waves and all reflected waves. The condition of resonance is derived from the expression of steady-state response, from which natural frequencies and mode shapes can be obtained. A simply supported beam and a cantilever beam are used as examples to verify the concept of wave-mode duality at resonance. The wave-train closure principle is then examined. It is shown that the principle does not describe the realistic process of the formulation of a vibration mode in general. However, “virtual” waves are generated to show that the principle can be served as a technique to determine natural frequencies and mode shapes from the point of view of wave propagation.

2. Wave evolution in a beam

Consider a uniform beam of length L as shown in Fig. 1. According to the Timoshenko beam theory, the equation of motion is given by

$$\mathbf{D}w = \begin{Bmatrix} F(z, t) \\ 0 \end{Bmatrix}, \tag{1}$$

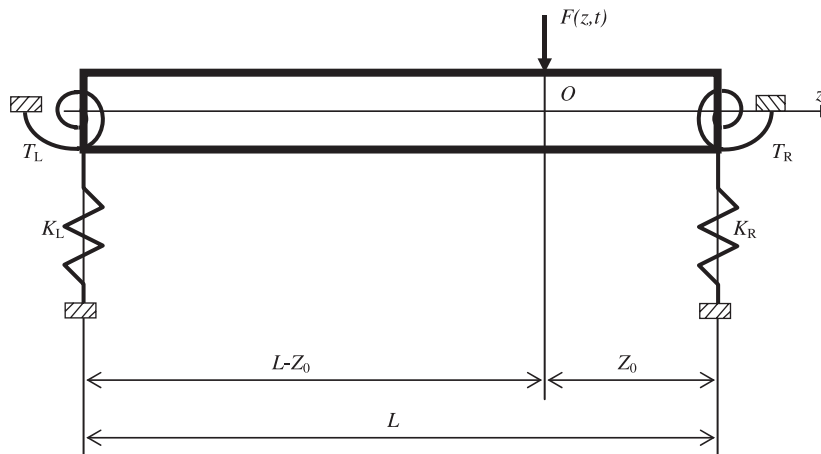


Fig. 1. A general elastically supported beam subjected to external force at an intermediate position.

where \mathbf{w} is a vector representing Timoshenko beam vibration, and \mathbf{D} is the corresponding operator, and $F(z, t)$ is the excitation force, given here as

$$F(z, t) = \begin{cases} F_0 e^{i\omega t} & \text{at } z = 0, \\ 0 & \text{otherwise.} \end{cases} \tag{2}$$

Instead of using the conventional expression

$$\mathbf{w}(z, t) = \begin{Bmatrix} w(z, t) \\ \phi(z, t) \end{Bmatrix},$$

a wave representation introduced by Wang and So [23] is used in the present paper. The beam motion \mathbf{w} is expressed as

$$\mathbf{w}(z, t) = \begin{Bmatrix} w_\phi(z, t) \\ w_\gamma(z, t) \end{Bmatrix} = \begin{Bmatrix} r \\ 1 \end{Bmatrix} w_\gamma(z, t),$$

where $w_\phi(z, t)$ and $w_\gamma(z, t)$ are transverse displacements due to bending rotation $\phi(z, t) = (\partial w_\phi(z, t))/\partial z$, and shear angle $\gamma(z, t) = (\partial w_\gamma(z, t))/\partial z$, respectively. The conventional expression is related to the present wave representation by

$$\begin{Bmatrix} w(z, t) \\ \phi(z, t) \end{Bmatrix} = \begin{Bmatrix} (1+r)w_\gamma(z, t) \\ \partial[(1+r)w_\gamma(z, t)]/\partial z \end{Bmatrix},$$

where $r = r_a = (c'_2/c_{pa})^2 - 1$ for the \mathbf{w}^{in} -wave and $r = r_b = (c'_2/c_{pb})^2 - 1$ for the \mathbf{w}^{out} -wave, $c_{pa} = \omega/k_a$ and $c_{pb} = \omega/k_b$ are phase velocities, and k_a and k_b are wavenumbers of the \mathbf{w}^{in} -wave and the \mathbf{w}^{out} -wave, respectively.

In Wang and So [23], it was shown that the shear deformation is either in-phase or out-of-phase with respect to the bending deformation, resulting in two types of flexural waves, the former corresponding to the k_a -wave and the latter to the k_b -wave as defined in Ref. [10]. These two types of waves were denoted as the \mathbf{w}^{in} -wave and the \mathbf{w}^{out} -wave, respectively, where “in” means “in-phase” while “out” means “out-of-phase”. This phenomenon was also found to be related to the entanglement of two standing waves in a Timoshenko beam [24]. At each frequency, \mathbf{w}^{in} -wave and \mathbf{w}^{out} -wave co-exist in an infinite beam. These two waves are said to be degenerate and can be expressed as

$$\begin{aligned} \mathbf{w}_\gamma(z, t) &= \{ \mathbf{w}^{\text{in}}(z, t) \quad \mathbf{w}^{\text{out}}(z, t) \} \\ &= \left\{ w_\gamma^{\text{in}}(z, t) \begin{pmatrix} 1 \\ 0 \end{pmatrix} \quad w_\gamma^{\text{out}}(z, t) \begin{pmatrix} 0 \\ 1 \end{pmatrix} \right\}. \end{aligned}$$

In Eq. (1), the operator \mathbf{D} is given by

$$\mathbf{D} = \begin{bmatrix} m \frac{\partial^2}{\partial t^2} & m \frac{\partial^2}{\partial t^2} - KGA \frac{\partial^2}{\partial z^2} \\ EI \frac{\partial^3}{\partial z^3} - J \frac{\partial^3}{\partial z \partial t^2} & KGA \frac{\partial}{\partial z} \end{bmatrix}, \tag{3}$$

where $m = \rho A$ and $J = \rho I$ are the mass and the mass moment of inertia per unit length of the beam, respectively, ρ is the density, K is the shear coefficient, I , A , E and G are the second moment of area and of cross-sectional area, the Young’s modulus and shear modulus, respectively.

The continuous sinusoidal force excitation is assumed to be applied at the origin $z = 0$, which is Z_0 away from the right boundary of the beam. The excitation, expressed as $F = F_0 e^{i\omega t}$, produces a forward propagating wave and a backward propagating wave, expressed as

$$\begin{aligned} \pm \mathbf{w}_\gamma(z, t) &= \left\{ \pm w_\gamma^{\text{in}}(z, t) \begin{pmatrix} 1 \\ 0 \end{pmatrix} \quad \pm w_\gamma^{\text{out}}(z, t) \begin{pmatrix} 0 \\ 1 \end{pmatrix} \right\} = \left\{ \pm w_\gamma^{\text{in}}(z) \begin{pmatrix} 1 \\ 0 \end{pmatrix} \quad \pm w_\gamma^{\text{out}}(z) \begin{pmatrix} 0 \\ 1 \end{pmatrix} \right\} e^{i\omega t} \\ &= \left(\pm W_{\gamma 0}^{\text{in}} e^{\mp i k_a z} \begin{pmatrix} 1 \\ 0 \end{pmatrix} \quad (-\pm W_{\gamma 0}^{\text{out}}) e^{\mp i k_b z} \begin{pmatrix} 0 \\ 1 \end{pmatrix} \right) e^{i\omega t}, \end{aligned} \tag{4}$$

where ω is the frequency of excitation, and the subscripts ‘+’ and ‘-’ represent forward and backward propagating waves, respectively. Based on the analysis of Mead [25], the amplitudes of the initial waves given in Eq. (4) can be obtained. The results are

$$\pm \mathbf{W}_{\gamma 0}^{\text{in}} = \pm \mathbf{W}_{\gamma 0}^{\text{in}} = \pm \frac{F_0}{2KGA} \cdot \frac{r_b}{k_a(r_b - r_a)}, \tag{5a}$$

$$\pm \mathbf{W}_{\gamma 0}^{\text{out}} = \pm \mathbf{W}_{\gamma 0}^{\text{out}} = \pm \frac{F_0}{2KGA} \cdot \frac{r_a}{k_b(r_b - r_a)}. \tag{5b}$$

From the point of view of wave propagation, the steady-state response is the addition of all waves in the beam due to reflections at both boundaries, and can be obtained by tracing the process of wave propagation and reflection. Since wave reflection can be in the superposition or the degenerate state, the formulation of steady-state response for these two cases should be analyzed separately. It should be noted that the \mathbf{w}^{out} -wave below the critical frequency is evanescent. However, it can be treated as a special propagating wave with imaginary phase velocity.

2.1. Wave evolution in the superposed state

In this section, wave evolution in the superposition state is considered. Initially, a forward propagating wave and a backward propagating wave at time $t = 0$ due to the excitation is assumed. These waves are given by

$$\begin{aligned} +w_{\gamma 0} &= \left\{ +w_\gamma^{\text{in}} \begin{pmatrix} 1 \\ 0 \end{pmatrix} \quad +w_\gamma^{\text{out}} \begin{pmatrix} 0 \\ 1 \end{pmatrix} \right\}_0 u(t) \\ &= \begin{cases} \left(+\mathbf{W}_{\gamma 0}^{\text{in}} e^{-i k_a z} \begin{pmatrix} 1 \\ 0 \end{pmatrix} \quad (-+\mathbf{W}_{\gamma 0}^{\text{out}}) e^{-i k_b z} \begin{pmatrix} 0 \\ 1 \end{pmatrix} \right) e^{i\omega t} u(t), & 0 \leq z \leq Z_0, \\ 0 \quad -(\mathbf{L} - Z_0) \leq z < 0 \end{cases} \end{aligned} \tag{6a}$$

and

$$\begin{aligned}
 -w_{\gamma 0} &= \left\{ -w_{\gamma}^{\text{in}} \begin{pmatrix} 1 \\ 0 \end{pmatrix} \quad -w_{\gamma}^{\text{out}} \begin{pmatrix} 0 \\ 1 \end{pmatrix} \right\}_0 u(t) \\
 &= \begin{cases} \left(-\mathbf{W}_{\gamma 0}^{\text{in}} e^{ik_a z} \begin{pmatrix} 1 \\ 0 \end{pmatrix} \quad (-\mathbf{W}_{\gamma 0}^{\text{out}}) e^{ik_b z} \begin{pmatrix} 0 \\ 1 \end{pmatrix} \right) e^{i\omega t} u(t), & -(\mathbf{L} - Z_0) \leq z \leq 0, \\ 0 & 0 < z \leq Z_0, \end{cases} \quad (6b)
 \end{aligned}$$

where the subscript ‘0’ indicates initial waves, and $u(t)$ is the step function. The subsequent behavior of wave reflection at both ends of the beam is illustrated in Fig. 2. Since \mathbf{w}^{in} -wave and \mathbf{w}^{out} -wave have different phase velocity, they arrive and reflect at the boundary at different time, as indicated in the figure.

Firstly, consider wave reflection at the right boundary of the beam. The incident $+\mathbf{w}^{\text{out}}$ -wave is expressed as

$$+\mathbf{w}^{\text{out}}(z, t) = (-+\mathbf{W}_{\gamma 0}^{\text{out}}) \begin{pmatrix} 0 \\ 1 \end{pmatrix} e^{i(\omega t - k_b z)} u\left(t - \frac{z}{c_{pb}}\right). \quad (7)$$

In general, the reflected wave is the superposition of a $-\mathbf{w}^{\text{in}}$ component and a $-\mathbf{w}^{\text{out}}$ component, written as

$$[-\mathbf{w}(z, t)]_{o1} = \begin{pmatrix} -w_{\gamma}^{\text{in}} \\ -w_{\gamma}^{\text{out}} \end{pmatrix}_{o1} = \begin{pmatrix} (-W_{\gamma 0}^{\text{in}})_{o1} e^{i(\omega t + k_a z)} u\left(t - \frac{Z_0}{c_{pb}} - \frac{Z_0 - z}{c_{pa}}\right) \\ (-W_{\gamma 0}^{\text{out}})_{o1} e^{i(\omega t + k_b z)} u\left(t - \frac{Z_0}{c_{pb}} - \frac{Z_0 - z}{c_{pb}}\right) \end{pmatrix}, \quad (8)$$

where the number in the subscript indicates the round of wave reflection, and the alphabet ‘o’ indicates the source of the reflected waves is a \mathbf{w}^{out} -wave. The amplitudes of the reflected waves can be written as

$$\begin{pmatrix} (-W_{\gamma 0}^{\text{in}})_{o1} \\ (-W_{\gamma 0}^{\text{out}})_{o1} \end{pmatrix} = \begin{pmatrix} \tilde{r}_{12R} \\ \tilde{r}_{22R} \end{pmatrix} (-+\mathbf{W}_{\gamma 0}^{\text{out}}), \quad (9)$$

where \tilde{r}_{12R} and \tilde{r}_{22R} are wave reflection coefficients. For the forward propagating \mathbf{w}^{in} -wave, the behavior of wave reflection is similar, given by

$$[-\mathbf{w}(z, t)]_{i1} = \begin{pmatrix} -w_{\gamma}^{\text{in}} \\ -w_{\gamma}^{\text{out}} \end{pmatrix}_{i1} = \begin{pmatrix} (-W_{\gamma 0}^{\text{in}})_{i1} e^{i(\omega t + k_a z)} u\left(t - \frac{Z_0}{c_{pa}} - \frac{Z_0 - z}{c_{pa}}\right) \\ (-W_{\gamma 0}^{\text{out}})_{i1} e^{i(\omega t + k_b z)} u\left(t - \frac{Z_0}{c_{pa}} - \frac{Z_0 - z}{c_{pb}}\right) \end{pmatrix}. \quad (10)$$

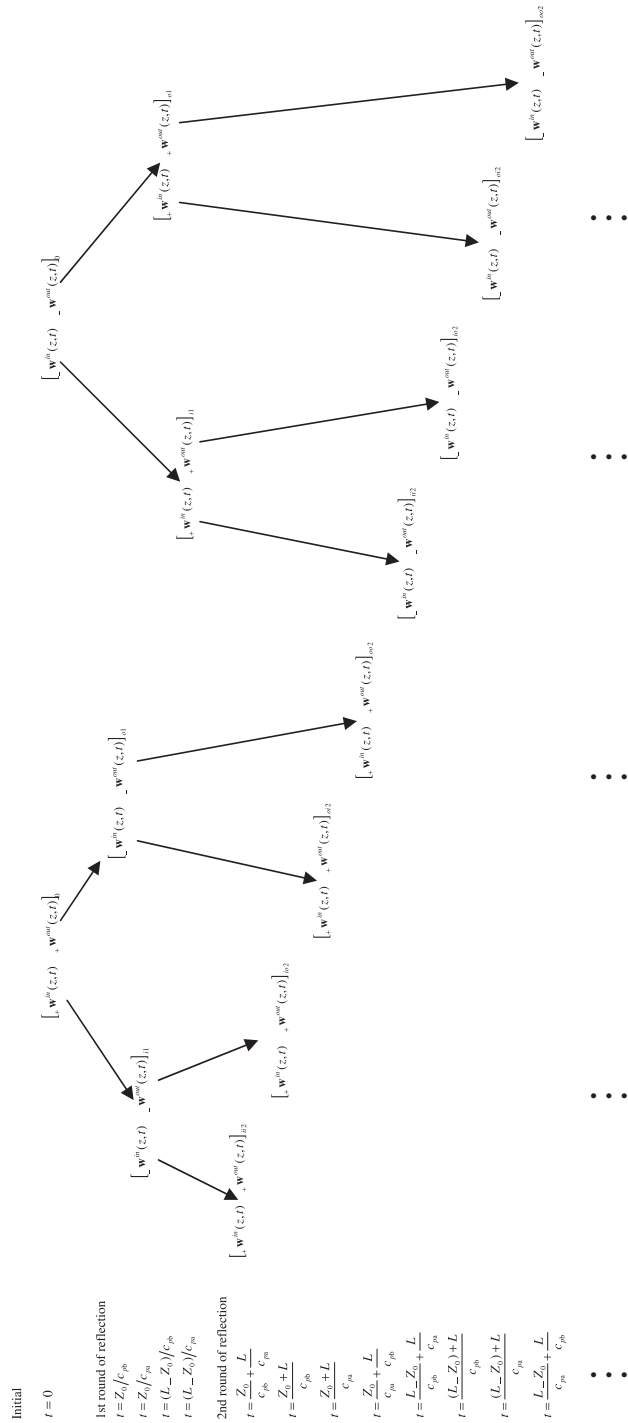


Fig. 2. Illustration of wave evolution in the superposition state.

The amplitudes of the reflected waves can be written as

$$\begin{pmatrix} (-W_{\gamma 0}^{\text{in}})_{i1} \\ (-W_{\gamma 0}^{\text{out}})_{i1} \end{pmatrix} = \begin{pmatrix} \tilde{r}_{11R} \\ \tilde{r}_{21R} \end{pmatrix} (+W_{\gamma 0}^{\text{in}}), \quad (11)$$

where \tilde{r}_{12R} and \tilde{r}_{22R} are wave reflection coefficients.

In the present wave evolution analysis, the steady-state response is of primary concern, that is, the waves are considered only after a sufficiently long time, when all step functions in the wave expressions take the value of unity. The reflected waves can thus be combined and written in the matrix form as

$$-\mathbf{w}_{\gamma 1} == \begin{pmatrix} -W_{\gamma}^{\text{in}} \\ -W_{\gamma}^{\text{out}} \end{pmatrix}_1 = \begin{pmatrix} -W_{\gamma 0,1}^{\text{in}} e^{i(\omega t + k_a z)} \\ -W_{\gamma 0,1}^{\text{out}} e^{i(\omega t + k_b z)} \end{pmatrix}. \quad (12)$$

The amplitudes of the reflected waves are given by

$$\begin{pmatrix} -W_{\gamma 0,1}^{\text{in}} \\ -W_{\gamma 0,1}^{\text{out}} \end{pmatrix} = [\tilde{\mathbf{R}}_R] \begin{pmatrix} +W_{\gamma 0}^{\text{in}} \\ (-+W_{\gamma 0}^{\text{out}}) \end{pmatrix} = \mathbf{T}_{0R} [\mathbf{R}_R] \mathbf{T}_{0R} \begin{pmatrix} +W_{\gamma 0}^{\text{in}} \\ (-+W_{\gamma 0}^{\text{out}}) \end{pmatrix}, \quad (13)$$

where

$$\mathbf{T}_{0R} = \begin{pmatrix} e^{-ik_a Z_0} & 0 \\ 0 & e^{-ik_b Z_0} \end{pmatrix},$$

\mathbf{R}_R is the wave reflection matrix given by Wang and So [23], as listed in the appendix.

Similarly, at the left boundary $z = -(L - Z_0)$, the reflected waves can be expressed as

$$+\mathbf{w}_{\gamma 1} == \begin{pmatrix} +W_{\gamma}^{\text{in}} \\ +W_{\gamma}^{\text{out}} \end{pmatrix}_1 = \begin{pmatrix} +W_{\gamma 0,1}^{\text{in}} e^{i(\omega t - k_a z)} \\ +W_{\gamma 0,1}^{\text{out}} e^{i(\omega t - k_b z)} \end{pmatrix}. \quad (14)$$

The amplitudes of the reflected waves are given by

$$\begin{pmatrix} +W_{\gamma 0,1}^{\text{in}} \\ +W_{\gamma 0,1}^{\text{out}} \end{pmatrix} = [\tilde{\mathbf{R}}_L] \begin{pmatrix} -W_{\gamma 0}^{\text{in}} \\ (- -W_{\gamma 0}^{\text{out}}) \end{pmatrix} = \mathbf{T}_{0L} [\mathbf{R}_L] \mathbf{T}_{0L} \begin{pmatrix} -W_{\gamma 0}^{\text{in}} \\ (- -W_{\gamma 0}^{\text{out}}) \end{pmatrix}, \quad (15)$$

where

$$\mathbf{T}_{0L} = \begin{pmatrix} e^{-ik_a(L-Z_0)} & 0 \\ 0 & e^{-ik_b(L-Z_0)} \end{pmatrix},$$

\mathbf{R}_L is the wave reflection matrix [23] listed in the appendix.

The reflected waves given by Eqs. (12) and (14) will produce more reflected waves in the second round of wave reflection as shown in Fig. 2. Analogous to the above analysis, the reflected waves

can be written in the matrix form. At the right boundary $z = Z_0$, they are expressed as

$$-\mathbf{w}_{\gamma 2} = \begin{pmatrix} -W_{\gamma}^{\text{in}} \\ -W_{\gamma}^{\text{out}} \end{pmatrix}_2 = \begin{pmatrix} -W_{\gamma 0,2}^{\text{in}} e^{i(\omega t + k_a z)} \\ -W_{\gamma 0,2}^{\text{out}} e^{i(\omega t + k_b z)} \end{pmatrix}, \tag{16}$$

where

$$\begin{pmatrix} -W_{\gamma 0,2}^{\text{in}} \\ -W_{\gamma 0,2}^{\text{out}} \end{pmatrix} = [\tilde{\mathbf{R}}_R][\tilde{\mathbf{R}}_L] \begin{pmatrix} -W_{\gamma 0}^{\text{in}} \\ (-W_{\gamma 0}^{\text{out}}) \end{pmatrix}.$$

At the left boundary $z = -(L - Z_0)$, they are expressed as

$$+\mathbf{w}_{\gamma 2} = \begin{pmatrix} +W_{\gamma}^{\text{in}} \\ +W_{\gamma}^{\text{out}} \end{pmatrix}_2 = \begin{pmatrix} +W_{\gamma 0,2}^{\text{in}} e^{i(\omega t - k_a z)} \\ +W_{\gamma 0,2}^{\text{out}} e^{i(\omega t - k_b z)} \end{pmatrix}, \tag{17}$$

where

$$\begin{pmatrix} +W_{\gamma 0,2}^{\text{in}} \\ +W_{\gamma 0,2}^{\text{out}} \end{pmatrix} = [\tilde{\mathbf{R}}_L][\tilde{\mathbf{R}}_R] \begin{pmatrix} +W_{\gamma 0}^{\text{in}} \\ (-+W_{\gamma 0}^{\text{out}}) \end{pmatrix}.$$

In order to obtain a compact expression for the reflected waves, the forward and backward wave units are defined here as

$$[+\mathbf{w}_{\gamma}]_{\text{unit}} = \begin{pmatrix} +W_{\gamma}^{\text{in}} \\ +W_{\gamma}^{\text{out}} \end{pmatrix}_{\text{unit}} = [+\mathbf{w}_{\gamma 0}] + [-\mathbf{w}_{\gamma 1}] + [+\mathbf{w}_{\gamma 2}], \tag{18a}$$

$$[-\mathbf{w}_{\gamma}]_{\text{unit}} = \begin{pmatrix} -W_{\gamma}^{\text{in}} \\ -W_{\gamma}^{\text{out}} \end{pmatrix}_{\text{unit}} = [-\mathbf{w}_{\gamma 0}] + [+\mathbf{w}_{\gamma 1}] + [-\mathbf{w}_{\gamma 2}]. \tag{18b}$$

It should be noted that the initial waves, $+\mathbf{w}_{\gamma 0}$ and $-\mathbf{w}_{\gamma 0}$, are defined at one part of the beam only, as shown by Eqs. (6a) and (6b). Correspondingly, $+\mathbf{w}_{\gamma 2}$ and $-\mathbf{w}_{\gamma 2}$, are defined at $0 < z \leq Z_0$ and $-(L - Z_0) \leq z < 0$, respectively. Thus defined, each of the wave units would cover the whole beam span, as illustrated in Fig. 3.

In terms of the wave units, the response of the beam is obtained by the addition of the initial propagating waves and all reflected waves, expressed as

$$\begin{pmatrix} W_{\gamma}^{\text{in}} \\ W_{\gamma}^{\text{out}} \end{pmatrix} = \left[\sum_{m=0}^M ([\tilde{\mathbf{R}}_L][\tilde{\mathbf{R}}_R])^m \right] [+\mathbf{w}_{\gamma}]_{\text{unit}} + \left[\sum_{m=0}^M ([\tilde{\mathbf{R}}_R][\tilde{\mathbf{R}}_L])^m \right] [-\mathbf{w}_{\gamma}]_{\text{unit}}, \tag{19}$$

where M is the number of times for the initial wave to be reflected at the left and right boundaries.

The steady state is achieved when $M \rightarrow \infty$, and Eq. (19) becomes

$$\begin{pmatrix} W_{\gamma}^{\text{in}} \\ W_{\gamma}^{\text{out}} \end{pmatrix} \stackrel{M \rightarrow \infty}{\equiv} (\mathbf{I} - [\tilde{\mathbf{R}}_L][\tilde{\mathbf{R}}_R])^{-1} [+\mathbf{w}_{\gamma}]_{\text{unit}} + (\mathbf{I} - [\tilde{\mathbf{R}}_R][\tilde{\mathbf{R}}_L])^{-1} [-\mathbf{w}_{\gamma}]_{\text{unit}}. \tag{20}$$

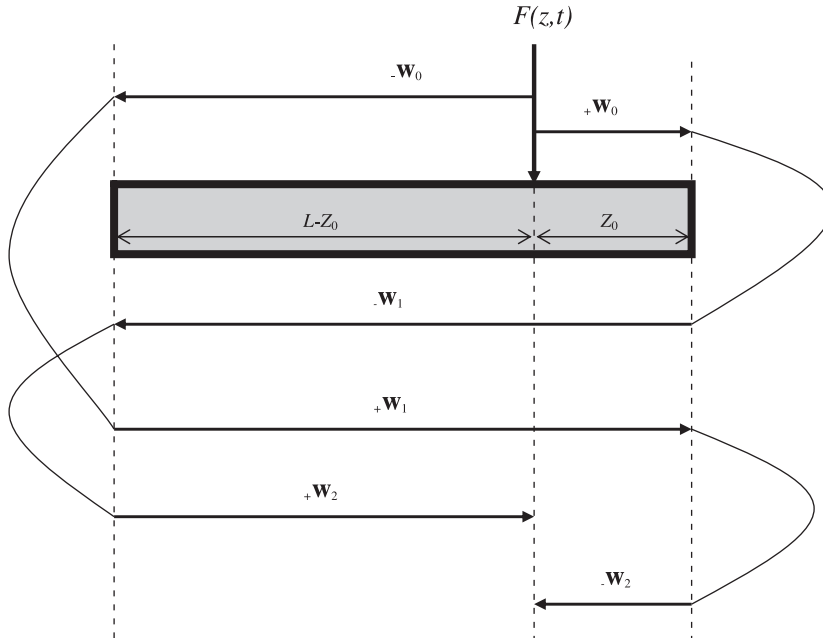


Fig. 3. Illustration of the “wave units”.

At resonance, the amplitude of the steady-state response should be infinity. This is accomplished if

$$|\mathbf{I} - [\tilde{\mathbf{R}}_L][\tilde{\mathbf{R}}_R]| = |\mathbf{I} - [\tilde{\mathbf{R}}_R][\tilde{\mathbf{R}}_L]| = 0. \tag{21}$$

Eq. (21) is the frequency equation from which natural frequencies are calculated.

In order to derive the expression of the associated mode shape, denote

$$\mathbf{I} - [\tilde{\mathbf{R}}_L][\tilde{\mathbf{R}}_R] = \begin{pmatrix} m_{11} & m_{12} \\ m_{21} & m_{22} \end{pmatrix}, \quad \mathbf{I} - [\tilde{\mathbf{R}}_R][\tilde{\mathbf{R}}_L] = \begin{pmatrix} n_{11} & n_{12} \\ n_{21} & n_{22} \end{pmatrix}. \tag{22}$$

Then

$$(\mathbf{I} - [\tilde{\mathbf{R}}_L][\tilde{\mathbf{R}}_R])^{-1} = \frac{1}{\begin{vmatrix} m_{11} & m_{12} \\ m_{21} & m_{22} \end{vmatrix}} \begin{pmatrix} m_{22} & -m_{12} \\ -m_{21} & m_{11} \end{pmatrix}, \tag{23a}$$

$$(\mathbf{I} - [\tilde{\mathbf{R}}_R][\tilde{\mathbf{R}}_L])^{-1} = \frac{1}{\begin{vmatrix} n_{11} & n_{12} \\ n_{21} & n_{22} \end{vmatrix}} \begin{pmatrix} n_{22} & -n_{12} \\ -n_{21} & n_{11} \end{pmatrix}. \tag{23b}$$

At resonance, $1 / \begin{vmatrix} m_{11} & m_{12} \\ m_{21} & m_{22} \end{vmatrix} = \infty$ and $1 / \begin{vmatrix} n_{11} & n_{12} \\ n_{21} & n_{22} \end{vmatrix} = \infty$, the steady-state response is then given by

$$\begin{pmatrix} w_\gamma^{\text{in}} \\ w_\gamma^{\text{out}} \end{pmatrix} = \infty \cdot \left[\begin{pmatrix} m_{22} & -m_{12} \\ -m_{21} & m_{11} \end{pmatrix} [{}_+\mathbf{w}_\gamma]_{\text{unit}} + \begin{pmatrix} n_{22} & -n_{12} \\ -n_{21} & n_{11} \end{pmatrix} [{}_-\mathbf{w}_\gamma]_{\text{unit}} \right]. \quad (24)$$

The mode shape can thus be deduced from Eq. (24) and is given by

$$\begin{aligned} \begin{pmatrix} w_\gamma^{\text{in}}(z) \\ -w_\gamma^{\text{out}}(z) \end{pmatrix} &= \begin{pmatrix} m_{22} & -m_{12} \\ -m_{21} & m_{11} \end{pmatrix} \begin{pmatrix} +w_\gamma^{\text{in}}(z) \\ +w_\gamma^{\text{out}}(z) \end{pmatrix}_{\text{unit}} \quad \text{or} \\ \begin{pmatrix} w_\gamma^{\text{in}}(z) \\ -w_\gamma^{\text{out}}(z) \end{pmatrix} &= \begin{pmatrix} n_{22} & -n_{12} \\ -n_{21} & n_{11} \end{pmatrix} \begin{pmatrix} -w_\gamma^{\text{in}}(z) \\ -w_\gamma^{\text{out}}(z) \end{pmatrix}_{\text{unit}}, \end{aligned} \quad (25)$$

where $\begin{pmatrix} +w_\gamma^{\text{in}}(z) \\ +w_\gamma^{\text{out}}(z) \end{pmatrix}_{\text{unit}}$ and $\begin{pmatrix} -w_\gamma^{\text{in}}(z) \\ -w_\gamma^{\text{out}}(z) \end{pmatrix}_{\text{unit}}$ are spatial parts of the wave units.

At this stage, it would be of interest to compare the frequency equations obtained by the present analysis and using the wave-train closure principle. The latter frequency equation can be written in terms of the present nomenclature and is given by

$$|\mathbf{I} - [\mathbf{T}_{L0}][\mathbf{R}_L][\mathbf{T}_{RL}][\mathbf{R}_R][\mathbf{T}_{0R}]| = 0. \quad (26)$$

The relations between the wave reflection matrices $\tilde{\mathbf{R}}_L$, $\tilde{\mathbf{R}}_R$ and \mathbf{R}_L , \mathbf{R}_R are expressed as

$$\tilde{\mathbf{R}}_L = [\mathbf{T}_{0L}][\mathbf{R}_L][\mathbf{T}_{0L}], \quad (27a)$$

$$\tilde{\mathbf{R}}_R = [\mathbf{T}_{0R}][\mathbf{R}_R][\mathbf{T}_{0R}]. \quad (27b)$$

Substituting Eqs. (27a) and (27b) into Eq. (21), the following is obtained:

$$|\mathbf{I} - [\mathbf{T}_{0L}][\mathbf{R}_L][\mathbf{T}_{0L}][\mathbf{T}_{0R}][\mathbf{R}_R][\mathbf{T}_{0R}]| = 0. \quad (28)$$

Therefore, noting that $[\mathbf{T}_{0L}][\mathbf{T}_{0R}] = [\mathbf{T}_{RL}]$ and $[\mathbf{T}_{0L}] = [\mathbf{T}_{L0}]$, Eqs. (28) and (26) become identical.

2.2. Wave evolution in the degenerate state

In the above section, wave evolution in the superposition state is investigated, and the steady-state response is obtained. It should be noted, however, the two waves can be reflected independently at a specific frequency

$$\omega_{\text{spe}} = \sqrt{\frac{K_{z_0} T_{z_0}}{KGA \cdot EI}} c'_2$$

for a general elastically supported boundary or at all frequencies for a simply supported or a sliding boundary [10,23], that is, the two waves remain degenerate upon reflection.

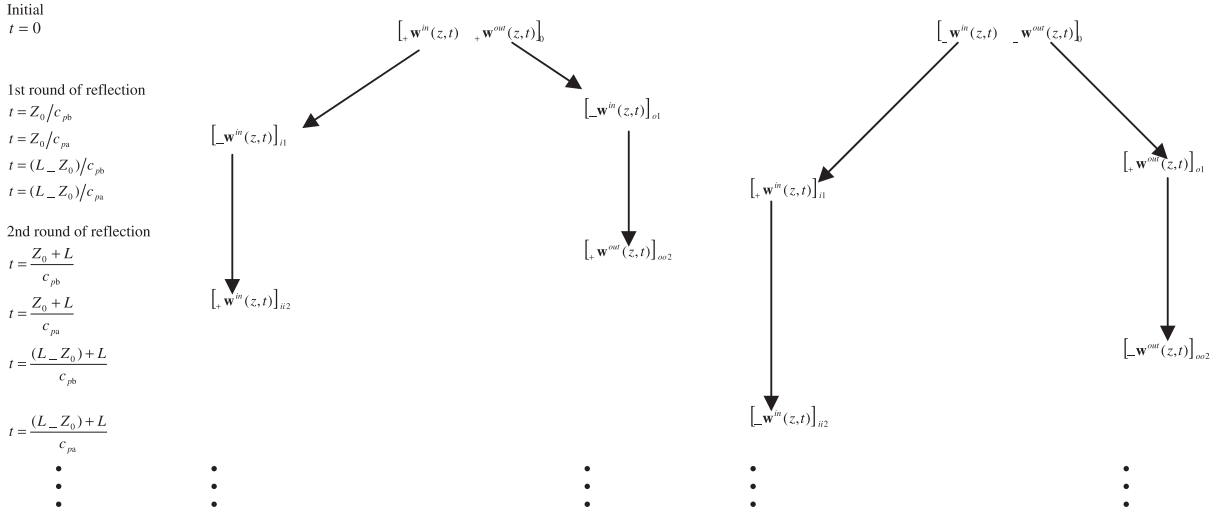


Fig. 4. Illustration of wave evolution in the degenerate state.

In the degenerate state, the process of wave evolution is shown in Fig. 4. The wave reflection matrices in this state are diagonal, written as

$$\tilde{\mathbf{R}}_L = \begin{pmatrix} r_{11L}e^{-ik_aL} & 0 \\ 0 & r_{22L}e^{-ik_bL} \end{pmatrix} \quad \text{and} \quad \tilde{\mathbf{R}}_R = \begin{pmatrix} r_{11R}e^{-ik_aL} & 0 \\ 0 & r_{22R}e^{-ik_bL} \end{pmatrix}, \quad (29)$$

where

$$r_{11L} = -e^{i\theta^{in}}, \quad r_{11R} = -e^{-i\theta^{in}}, \quad r_{22L} = -e^{i\theta^{out}},$$

$$r_{22R} = -e^{-i\theta^{out}}, \quad \theta^{in} = 2\text{arctg}\left(\frac{c_{pa}}{c'^2_2} \sqrt{\frac{T_{z_0} \cdot KGA}{EI \cdot K_{z_0}}}\right),$$

and

$$\theta^{out} = 2\text{arctg}\left(\frac{c_{pb}}{c'^2_2} \sqrt{\frac{T_{z_0} \cdot KGA}{EI \cdot K_{z_0}}}\right).$$

The wave units defined in Eqs. (18a) and (18b) become, in the degenerate state,

$$\begin{aligned} (+w^{\text{in}}_\gamma)_{\text{unit}} &= (+w^{\text{in}}_\gamma)_0 + (-w^{\text{in}}_\gamma)_1 + (+w^{\text{in}}_\gamma)_2 \\ &= (+W^{\text{in}}_{\gamma 0}) \left[(1 + e^{-i2k_aL})e^{-ik_az} - e^{-i\theta^{\text{in}}} e^{-i2k_aZ_0} e^{ik_az} \right] e^{i\omega t}, \end{aligned} \quad (30a)$$

$$\begin{aligned} (-w^{\text{in}}_\gamma)_{\text{unit}} &= (-w^{\text{in}}_\gamma)_0 + (+w^{\text{in}}_\gamma)_1 + (-w^{\text{in}}_\gamma)_2 \\ &= (-W^{\text{in}}_{\gamma 0}) \left[(1 + e^{i2k_aL})e^{ik_az} - e^{i\theta^{\text{in}}} e^{-i2k_a(L-Z_0)} e^{-ik_az} \right] e^{i\omega t}, \end{aligned} \quad (30b)$$

$$\begin{aligned} \left(+w_\gamma^{\text{out}}\right)_{\text{unit}} &= \left(+w_\gamma^{\text{out}}\right)_0 + \left(-w_\gamma^{\text{out}}\right)_1 + \left(+w_\gamma^{\text{out}}\right)_2 \\ &= \left(+W_{\gamma 0}^{\text{out}}\right) \left[\left(1 + e^{-i2k_b L}\right) e^{-ik_b z} - e^{-i\theta^{\text{out}}} e^{-i2k_b Z_0} e^{ik_b z} \right] e^{i\omega t}, \end{aligned} \tag{30c}$$

$$\begin{aligned} \left(-w_\gamma^{\text{out}}\right)_{\text{unit}} &= \left(-w_\gamma^{\text{out}}\right)_0 + \left(+w_\gamma^{\text{out}}\right)_1 + \left(-w_\gamma^{\text{out}}\right)_2 \\ &= \left(-W_{\gamma 0}^{\text{out}}\right) \left[\left(1 + e^{i2k_b L}\right) e^{ik_b z} - e^{i\theta^{\text{out}}} e^{-i2k_b(L-Z_0)} e^{-ik_b z} \right] e^{i\omega t}. \end{aligned} \tag{30d}$$

Then

$$\mathbf{I} - [\tilde{\mathbf{R}}_L][\tilde{\mathbf{R}}_R] = \mathbf{I} - [\tilde{\mathbf{R}}_R][\tilde{\mathbf{R}}_L] = \begin{pmatrix} 1 - e^{-i2k_a L} & 0 \\ 0 & 1 - e^{-i2k_b L} \end{pmatrix}. \tag{31}$$

The steady-state response in the degenerate state is expressed as

$$\begin{aligned} \left\{ w_\gamma^{\text{in}} \begin{pmatrix} 1 \\ 0 \end{pmatrix} \quad w_\gamma^{\text{out}} \begin{pmatrix} 0 \\ 1 \end{pmatrix} \right\} \xrightarrow{M \rightarrow \infty} & \left\{ \left(\mathbf{I} - [\tilde{\mathbf{R}}_L][\tilde{\mathbf{R}}_R]\right)^{-1} \begin{pmatrix} +w_\gamma^{\text{in}} \\ 0 \end{pmatrix}_{\text{unit}} + \left(\mathbf{I} - [\tilde{\mathbf{R}}_R][\tilde{\mathbf{R}}_L]\right)^{-1} \begin{pmatrix} -w_\gamma^{\text{in}} \\ 0 \end{pmatrix}_{\text{unit}} \right. \\ & \left. \left(\mathbf{I} - [\tilde{\mathbf{R}}_L][\tilde{\mathbf{R}}_R]\right)^{-1} \begin{pmatrix} 0 \\ +w_\gamma^{\text{out}} \end{pmatrix}_{\text{unit}} + \left(\mathbf{I} - [\tilde{\mathbf{R}}_R][\tilde{\mathbf{R}}_L]\right)^{-1} \begin{pmatrix} 0 \\ -w_\gamma^{\text{out}} \end{pmatrix}_{\text{unit}} \right\}. \end{aligned} \tag{32}$$

It can be seen that the w^{in} - and the w^{out} -waves formulate vibration modes independently, that is, they do not interact as in the superposition state. Therefore, they can be written separately as

$$\begin{aligned} w_\gamma^{\text{in}} &= \frac{1}{1 - e^{-i2k_a L}} \left(+w_\gamma^{\text{in}}\right)_{\text{unit}} + \frac{1}{1 - e^{-i2k_a L}} \left(-w_\gamma^{\text{in}}\right)_{\text{unit}} \\ &= \frac{1}{1 - e^{-i2k_a L}} \left[\left(+w_\gamma^{\text{in}}\right)_{\text{unit}} + \left(-w_\gamma^{\text{in}}\right)_{\text{unit}} \right], \end{aligned} \tag{33a}$$

and

$$\begin{aligned} w_\gamma^{\text{out}} &= \frac{1}{1 - e^{-i2k_b L}} \left(+w_\gamma^{\text{out}}\right)_{\text{unit}} + \frac{1}{1 - e^{-i2k_b L}} \left(-w_\gamma^{\text{out}}\right)_{\text{unit}} \\ &= \frac{1}{1 - e^{-i2k_b L}} \left[\left(+w_\gamma^{\text{out}}\right)_{\text{unit}} + \left(-w_\gamma^{\text{out}}\right)_{\text{unit}} \right]. \end{aligned} \tag{33b}$$

At resonance, the amplitude of the steady-state response should be infinity. Referring to Eqs. (33a) and (33b), this condition of resonance yields

$$1 - e^{-i2k_a L} = 0, \tag{34a}$$

$$1 - e^{-i2k_b L} = 0. \tag{34b}$$

Eqs. (34a) and (34b) lead to

$$k_a L = n_a \pi, \quad n_a = 1, 2, 3, \dots, \tag{35a}$$

$$k_b L = n_b \pi, \quad n_b = 1, 2, 3, \dots \tag{35b}$$

The corresponding mode shapes are given by

$$w_\gamma^{\text{in}}(z) = \left[+w_\gamma^{\text{in}}(z) \right]_{\text{unit}} \quad \text{or} \quad w_\gamma^{\text{in}}(z) = \left[-w_\gamma^{\text{in}}(z) \right]_{\text{unit}}, \quad (36a)$$

$$w_\gamma^{\text{out}}(z) = \left[+w_\gamma^{\text{out}}(z) \right]_{\text{unit}} \quad \text{or} \quad w_\gamma^{\text{out}}(z) = \left[-w_\gamma^{\text{out}}(z) \right]_{\text{unit}}. \quad (36b)$$

Eqs. (35a) and (35b) give the condition for a mode to exist, while the natural frequency of such a mode is the specific frequency. At this specific frequency, a standing wave is formulated by the w^{in} - or the w^{out} -wave only, thus termed as *single* standing wave. If Eqs. (35a) and (35b) are satisfied simultaneously, a w^{in} - and a w^{out} -single standing wave exist at the same specific frequency, leading to a pair of *degenerate* standing waves. An additional condition given by

$$k_a/k_b = n_a/n_b, \quad n_a, n_b = 1, 2, 3, \dots, \quad (37)$$

must be satisfied. This condition is identical to the one obtained by using the wave-train closure principle [23]. It should be noted that a single standing wave or a pair of degenerate standing waves require that wave reflections at both boundaries should be in the degenerate state at the same specific frequency. Otherwise, a superposed standing wave will be formulated. Therefore, the condition $K_L T_L = K_R T_R$ must also be satisfied.

Two classical boundary conditions are worthy of further discussion. These are the simply supported and the sliding boundary conditions. For these two boundary conditions, wave reflection is in the degenerate state at all frequencies rather than at the specific frequency only. The condition of resonance and the mode shapes are still given by Eqs. (34a) and (34b), and (36a) and (36b), respectively. However, natural frequencies are determined by Eqs. (35a) and (35b) rather than given by the specific frequency. Consequently, a series of w^{in} -single standing waves and a series of w^{out} -single standing waves are formulated. Under certain conditions, a w^{in} - and a w^{out} -single standing wave is paired, yielding degenerated standing waves. This can be demonstrated by using the simply supported beam as an example. For such a beam, the reflection coefficients are written as $\tilde{r}_{11L} = -1$, $\tilde{r}_{11R} = -1$, $\tilde{r}_{22L} = -1$, and $\tilde{r}_{22R} = -1$. The condition of resonance yields

$$k_a L = n_a \pi, \quad n_a = 1, 2, 3, \dots, \quad (38a)$$

$$k_b L = n_b \pi, \quad n_b = 1, 2, 3, \dots \quad (38b)$$

Eqs. (38a) and (38b) are different from Eqs. (35a) and (35b) because they are frequency equations giving natural frequencies of the beam. In general, the modes associated with these natural frequencies are single standing waves. For a given beam length, there is one group of w^{in} -standing waves and one group of w^{out} -standing waves. Under certain conditions, a w^{in} -standing wave and a w^{out} -standing wave may exist at the same natural frequency to formulate a pair of degenerate standing waves. This is the same conclusion drawn from the analysis based on the wave-train closure principle.

3. Wave-mode duality in resonant beam vibration

A comparison of natural frequencies and mode shapes obtained by the present wave evolution analysis and the mode approach is carried out to further understand wave-mode duality in resonant beam vibration. The comparison is made separately for the degenerate and superposition state.

3.1. The degenerate state

The simply supported beam is used as an example of the degenerate state. Natural frequencies are calculated from the frequency Eqs. (38a) and (38b). It can be seen that they are identical to those derived by the mode approach (the method of modal analysis). Therefore, natural frequencies obtained by the present wave approach and the mode approach are identical.

The corresponding mode shapes are given by Eqs. (36a) and (36b). In order to compare them to the results by the mode approach, the mode shapes are expressed here as

$$w_\gamma^{\text{in}}(z) = \left[+w_\gamma^{\text{in}}(z) \right]_{\text{unit}} + \left[-w_\gamma^{\text{in}}(z) \right]_{\text{unit}}, \tag{39a}$$

$$w_\gamma^{\text{out}}(z) = \left[+w_\gamma^{\text{out}}(z) \right]_{\text{unit}} + \left[-w_\gamma^{\text{out}}(z) \right]_{\text{unit}}. \tag{39b}$$

Substituting the expressions of the wave units given by Eqs. (30a)–(30d) into Eqs. (39a) and (39b) gives

$$w_\gamma^{\text{in}}(z) = (-2i)(+W_{\gamma 0}^{\text{in}})\{2 \sin[k_a(z - Z_0)] \cos(k_a Z_0)\}, \tag{40a}$$

$$w_\gamma^{\text{out}}(z) = (-2i)(-+W_{\gamma 0}^{\text{out}})\{2 \sin[k_b(z - Z_0)] \cos(k_b Z_0)\}. \tag{40b}$$

Normalizing by the maximum value, the mode shapes are given by

$$w_\gamma^{\text{in}}(z) = \sin[k_a(z - Z_0)], \tag{41a}$$

$$w_\gamma^{\text{out}}(z) = \sin[k_b(z - Z_0)]. \tag{41b}$$

It can be seen that they are identical to the mode shapes obtained by using the mode approach. Thus, the wave-mode duality in the degenerate state of resonant beam vibration can be justified.

3.2. The superposition state

In the superposition state, natural frequencies of a beam are obtained by solving the frequency equation (21), and the associated mode shapes are given by Eq. (25). While the wave-mode duality in the degenerate state is readily justified analytically, numerical solutions have to be sought in order to demonstrate the wave-mode duality in the superposition state. A cantilever beam is used as an example where experimental measurements are also available for comparison. For the cantilever beam, $K_L = \infty$, $T_L = \infty$, $K_R = 0$, and $T_R = 0$, and the frequency equation (21) can be written as

$$|\mathbf{I} - [\tilde{\mathbf{R}}_L][\tilde{\mathbf{R}}_R]| = |\mathbf{I} - [\tilde{\mathbf{R}}_R][\tilde{\mathbf{R}}_L]| = 0, \tag{42}$$

where

$$[\tilde{\mathbf{R}}_L] = \begin{pmatrix} e^{-ik_a(L-Z_0)} & 0 \\ 0 & e^{-ik_b(L-Z_0)} \end{pmatrix} [\mathbf{R}_L],$$

$$[\tilde{\mathbf{R}}_R] = \begin{pmatrix} e^{-ik_a Z_0} & 0 \\ 0 & e^{-ik_b Z_0} \end{pmatrix} [\mathbf{R}_R],$$

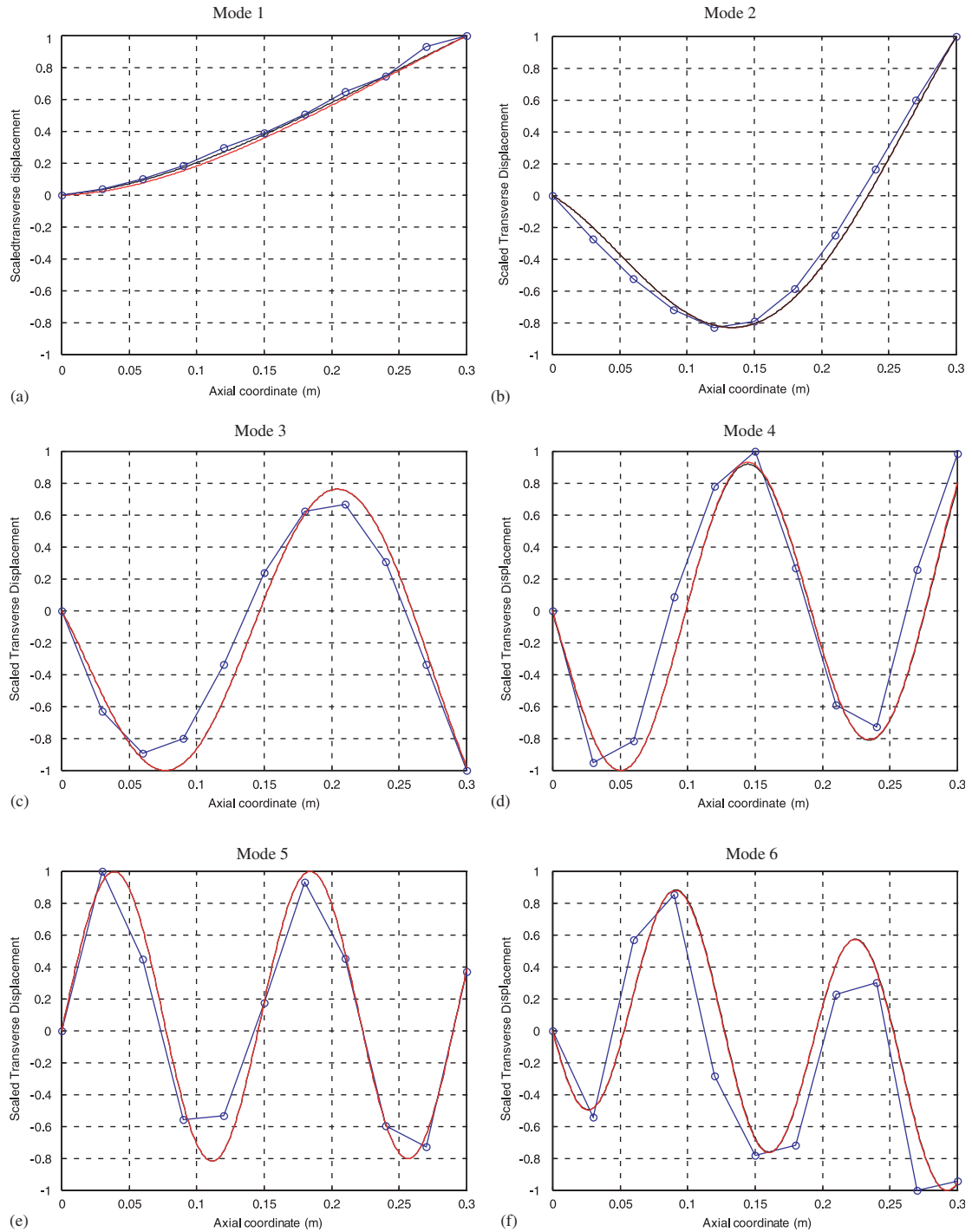


Fig. 5. Comparison of mode shapes of the first six modes of a cantilever beam. Solid and dotted lines are for calculated results by the present wave approach and the classical mode approach, respectively. Lines with symbol are for experimental measurements.

Table 1

Comparison of natural frequencies (Hz) of a cantilever beam obtained by the present wave approach, the mode approach [26] and experimental measurements [26]

Mode	Present wave approach	Mode approach [26]	Experimental measurements [26]
1	313.94	313.93	302.16
2	1520.09	1520.08	1473.6
3	3409.34	3409.32	3338.3
4	5376.27	5376.24	5292.0
5	7348.50	7348.46	7139.7
6	8197.93	8197.88	7828.2

$$\begin{aligned}
 \mathbf{R}_L &= - \begin{pmatrix} (r_a + 1) & (r_b + 1) \\ -r_a(ik_a) & -r_b(ik_b) \end{pmatrix}^{-1} \begin{pmatrix} (r_a + 1) & (r_b + 1) \\ -r_a(-ik_a) & -r_b(-ik_b) \end{pmatrix}, \\
 \mathbf{R}_R &= - \begin{pmatrix} -ik_a & -ik_b \\ -r_a k_a^2 & -r_b k_b^2 \end{pmatrix}^{-1} \begin{pmatrix} ik_a & ik_b \\ -r_a k_a^2 & -r_b k_b^2 \end{pmatrix}.
 \end{aligned} \tag{43}$$

The cantilever beam has a rectangular cross-section, 300 mm in length, 94 mm in height, and 18 mm in breadth. The material properties are as follows: ρ , the density is 1192 kg/m³, E , the Young’s modulus is 4.65 GPa, G , shear modulus is 2.32 GPa, and the shear coefficient is $\frac{5}{6}$. Further details of the experiment can be found in Ref. [26].

In Table 1, the natural frequencies calculated using the present wave approach and the mode approaches are listed, and the measured values are also given for comparison. It can be seen that the present wave approach and the mode approach yield the same predictions, which are in good agreement with experimental measurements. A comparison of mode shapes for total transverse displacement is given in Fig. 5, and good agreement is also obtained.

4. Further examination of the wave-train closure principle

In Section 2, it has been shown that the frequency equations obtained in the present study are identical to those derived using the wave-train closure principle. The wave-train closure principle can be considered as a description of the formulation of a vibration mode from the point of view of wave propagation. The present wave evolution results make it possible to examine the principle further on such a description. This is of interest because further physical understanding of the principle could be obtained. Again, the degenerate and superposition states are considered separately.

4.1. The degenerate state

The steady-state response in the degenerate state can be expressed as

$$\begin{Bmatrix} w_\gamma^{\text{in}} \\ w_\gamma^{\text{out}} \end{Bmatrix} \stackrel{M \rightarrow \infty}{\equiv} \begin{pmatrix} \frac{1}{1 - e^{-i2k_a L}} & 0 \\ 0 & \frac{1}{1 - e^{-i2k_b L}} \end{pmatrix} \left\{ \begin{pmatrix} +w_\gamma^{\text{in}} \\ +w_\gamma^{\text{out}} \end{pmatrix}_{\text{unit}} + \begin{pmatrix} -w_\gamma^{\text{in}} \\ -w_\gamma^{\text{out}} \end{pmatrix}_{\text{unit}} \right\}. \tag{44}$$

At resonance, the mode shape is given by

$$\begin{Bmatrix} w_\gamma^{\text{in}}(z) \\ w_\gamma^{\text{out}}(z) \end{Bmatrix} = \begin{pmatrix} 1 & 0 \\ 0 & 1 \end{pmatrix} \left\{ \begin{pmatrix} +w_\gamma^{\text{in}}(z) \\ +w_\gamma^{\text{out}}(z) \end{pmatrix}_{\text{unit}} + \begin{pmatrix} -w_\gamma^{\text{in}}(z) \\ -w_\gamma^{\text{out}}(z) \end{pmatrix}_{\text{unit}} \right\}, \tag{45}$$

where $\begin{pmatrix} +w_\gamma^{\text{in}}(z) \\ +w_\gamma^{\text{out}}(z) \end{pmatrix}_{\text{unit}}$ and $\begin{pmatrix} -w_\gamma^{\text{in}}(z) \\ -w_\gamma^{\text{out}}(z) \end{pmatrix}_{\text{unit}}$ are spatial parts of the wave units. It can be seen that the mode shape is determined by the wave units only.

According to the statement of the wave-train closure principle, in order to formulate a superposed standing wave, the wave units, $+w_{\gamma 2}$ and $-w_{\gamma 2}$ should close on $+w_{\gamma 0}$ and $-w_{\gamma 0}$, respectively. To further examine this statement, analytical expressions of wave units are considered. According to Eqs. (16) and (17),

$$-w_{\gamma 2} = \begin{pmatrix} -w_\gamma^{\text{in}} \\ -w_\gamma^{\text{out}} \end{pmatrix}_2 = \begin{pmatrix} -W_{\gamma 0,2}^{\text{in}} e^{i(\omega t + k_a z)} \\ -W_{\gamma 0,2}^{\text{out}} e^{i(\omega t + k_b z)} \end{pmatrix}, \tag{46a}$$

$$+w_{\gamma 2} = \begin{pmatrix} +w_\gamma^{\text{in}} \\ +w_\gamma^{\text{out}} \end{pmatrix}_2 = \begin{pmatrix} +W_{\gamma 0,2}^{\text{in}} e^{i(\omega t - k_a z)} \\ +W_{\gamma 0,2}^{\text{out}} e^{i(\omega t - k_b z)} \end{pmatrix}. \tag{46b}$$

In the degenerate state,

$$\begin{pmatrix} -W_{\gamma 0,2}^{\text{in}} \\ -W_{\gamma 0,2}^{\text{out}} \end{pmatrix} = [\tilde{\mathbf{R}}_R][\tilde{\mathbf{R}}_L] \begin{pmatrix} -W_{\gamma 0}^{\text{in}} \\ (-W_{\gamma 0}^{\text{out}}) \end{pmatrix} = \begin{pmatrix} -W_{\gamma 0}^{\text{in}} \\ (-W_{\gamma 0}^{\text{out}}) \end{pmatrix},$$

and

$$\begin{pmatrix} +W_{\gamma 0,2}^{\text{in}} \\ +W_{\gamma 0,2}^{\text{out}} \end{pmatrix} = [\tilde{\mathbf{R}}_L][\tilde{\mathbf{R}}_R] \begin{pmatrix} +W_{\gamma 0}^{\text{in}} \\ (+W_{\gamma 0}^{\text{out}}) \end{pmatrix} = \begin{pmatrix} +W_{\gamma 0}^{\text{in}} \\ (+W_{\gamma 0}^{\text{out}}) \end{pmatrix}.$$

Then,

$$+w_{\gamma 2} = +w_{\gamma 0}, \tag{47a}$$

$$-w_{\gamma 2} = -w_{\gamma 0}. \tag{47b}$$

From Eqs. (47a) and (47b), it can be seen that these two returning waves close on their initial waves, thus showing that the wave-train closure principle describes the realistic process of the formulation of a standing wave in the degenerate state.

4.2. The superposition state

A similar examination can be carried out for the formulation of a standing wave in the superposition state. Since analytical solutions are not available in the superposition state, again the cantilever beam in Section 3 is used as an example.

The wave units for the third mode of the cantilever beam are shown in Fig. 6. It can be seen that ${}_+w_{\gamma 2}$ does not close on ${}_+w_{\gamma 0}$ and ${}_-w_{\gamma 2}$ does not close on ${}_-w_{\gamma 0}$, thus showing that the wave-train closure principle does not hold in the superposition state. However, if “virtual” waves defined as

$$[{}_+\hat{w}_\gamma] = \begin{pmatrix} m_{22} & -m_{12} \\ -m_{21} & m_{11} \end{pmatrix} [{}_+w_\gamma], \tag{48a}$$

$$[{}_-\hat{w}_\gamma] = \begin{pmatrix} n_{22} & -n_{12} \\ -n_{21} & n_{11} \end{pmatrix} [{}_-w_\gamma], \tag{48b}$$

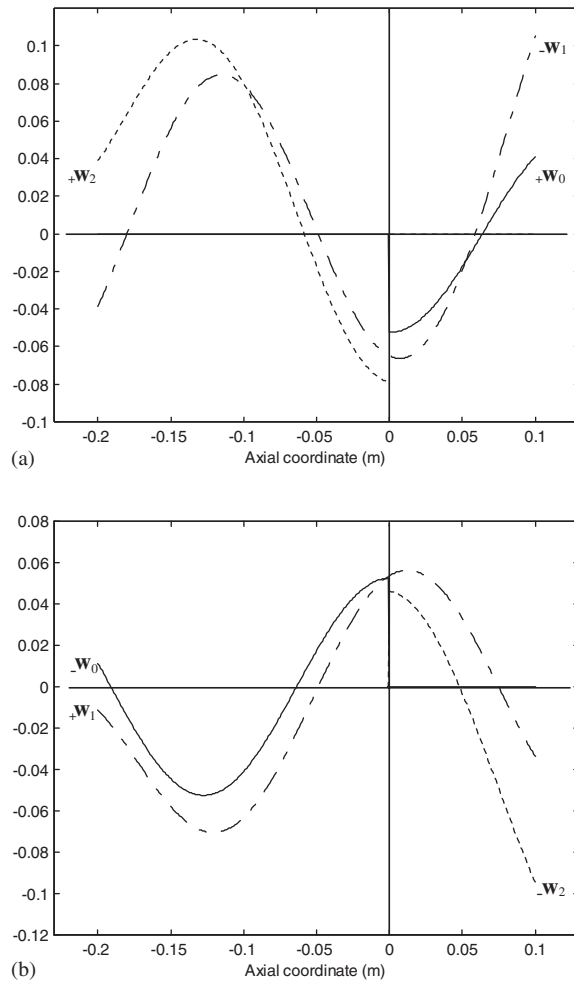


Fig. 6. Illustration of the waves in the wave units for the third mode of the cantilever beam: (a) ${}_+w_{unit}$ and (b) ${}_-w_{unit}$.

are introduced, then the corresponding “virtual” wave units are given by

$$\begin{aligned} [{}_{+}\hat{\mathbf{w}}_{\gamma}]_{\text{unit}} &= \begin{pmatrix} m_{22} & -m_{12} \\ -m_{21} & m_{11} \end{pmatrix} \{[{}_{+}\mathbf{w}_{\gamma 0}] + [{}_{-}\mathbf{w}_{\gamma 1}] + [{}_{+}\mathbf{w}_{\gamma 2}]\} \\ &= [{}_{+}\hat{\mathbf{w}}_{\gamma 0}] + [{}_{-}\hat{\mathbf{w}}_{\gamma 1}] + [{}_{+}\hat{\mathbf{w}}_{\gamma 2}], \end{aligned} \quad (49a)$$

$$\begin{aligned} [{}_{-}\hat{\mathbf{w}}_{\gamma}]_{\text{unit}} &= \begin{pmatrix} n_{22} & -n_{12} \\ -n_{21} & n_{11} \end{pmatrix} \{[{}_{-}\mathbf{w}_{\gamma 0}] + [{}_{+}\mathbf{w}_{\gamma 1}] + [{}_{-}\mathbf{w}_{\gamma 2}]\} \\ &= [{}_{-}\hat{\mathbf{w}}_{\gamma 0}] + [{}_{+}\hat{\mathbf{w}}_{\gamma 1}] + [{}_{-}\hat{\mathbf{w}}_{\gamma 2}]. \end{aligned} \quad (49b)$$

Noting that ${}_{+}\hat{\mathbf{w}}_{\gamma 2} = [\tilde{\mathbf{R}}_L][\tilde{\mathbf{R}}_R]{}_{+}\hat{\mathbf{w}}_{\gamma 0}$ and ${}_{-}\hat{\mathbf{w}}_{\gamma 2} = [\tilde{\mathbf{R}}_R][\tilde{\mathbf{R}}_L]({}_{-}\hat{\mathbf{w}}_{\gamma 0})$, it is not difficult to derive that

$${}_{+}\hat{\mathbf{w}}_{\gamma 2} = {}_{+}\hat{\mathbf{w}}_{\gamma 0}, \quad (50a)$$

$${}_{-}\hat{\mathbf{w}}_{\gamma 2} = -{}_{-}\hat{\mathbf{w}}_{\gamma 0}. \quad (50b)$$

From Eqs. (50a) and (50b), it can be seen that ${}_{+}\hat{\mathbf{w}}_{\gamma 2}$ closes on ${}_{+}\hat{\mathbf{w}}_{\gamma 0}$ and ${}_{-}\hat{\mathbf{w}}_{\gamma 2}$ closes on ${}_{-}\hat{\mathbf{w}}_{\gamma 0}$. In other words, the wave-train closure principle holds for the “virtual” waves. It should be noted that the “virtual” waves actually represent the steady-state waves after an infinite number of reflections at both boundaries. Such a state cannot be reached in reality, but can only be approached asymptotically. This suggests that the mode shapes measured experimentally are not perfect but approximate. However, after several rounds of reflections at both ends of the beam, the result of wave addition is already sufficient to yield a picture of mode shape with enough accuracy. This can be illustrated by the evolution of wave addition result given by Eq. (19).

From Eq. (19), the amplitude of total transverse displacement can be calculated as

$$W(z) = (1 + r_a)W_{\gamma}^{\text{in}}(z) + (1 + r_b)W_{\gamma}^{\text{out}}(z), \quad (51)$$

where $W_{\gamma}^{\text{in}}(z)$ and $W_{\gamma}^{\text{out}}(z)$ are spatial parts of $w_{\gamma}^{\text{in}}(z, t)$ and $w_{\gamma}^{\text{out}}(z, t)$ in Eq. (19). The calculated results at resonant frequencies of the third and the fourth modes as well as at an off-resonant frequency between them are plotted in Fig. 7. From the results at resonance, one can see that the shapes become smoother with the increment of M . At $M = 10$, the shapes can be said to be smooth enough. Meanwhile, it is seen that the result at the off-resonant frequency always has a discontinuity. One also notes that the variation of the shape at off-resonance is fluctuating rather than increasing monotonically at resonance. This is further studied by calculating the amplitude of total transverse displacement at the free end when the evolution continues, and the results are given in Fig. 8. It can be seen that the amplitude at resonance increases linearly and has a tendency to approach infinity when $M \rightarrow \infty$. At off-resonance, the amplitude is fluctuating and decreases gradually and appears to approach a finite value when $M \rightarrow \infty$.

It is noted that the amplitude of the final response is different from that of the initial response, because the final response is the addition of initial waves and all reflected waves, as shown by the wave evolution analysis. Hence, in general, the initial response is not equal to the final response.

The evolution from initial response to final steady-state response is a process of energy partition in the system. In the present study, the energy is continuously fed into the beam by external force. At resonance, the reflected waves are spatially synchronized with the initial waves; hence the final response becomes larger and larger, approaching infinity. At off-resonance, the condition of space

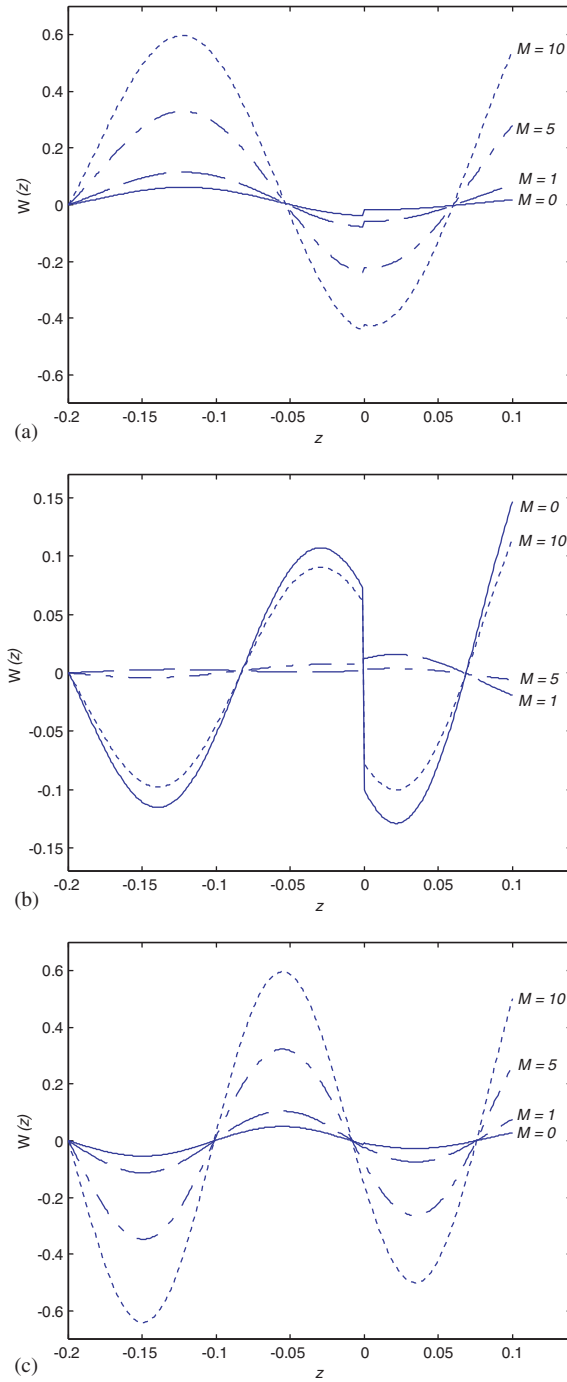


Fig. 7. Evolution of wave addition results: (a) at the resonant frequency of the third mode (3409 Hz); (b) at an off-resonant frequency between the third and the fourth modes (4400 Hz); and (c) at the resonant frequency of the fourth mode (5376 Hz).

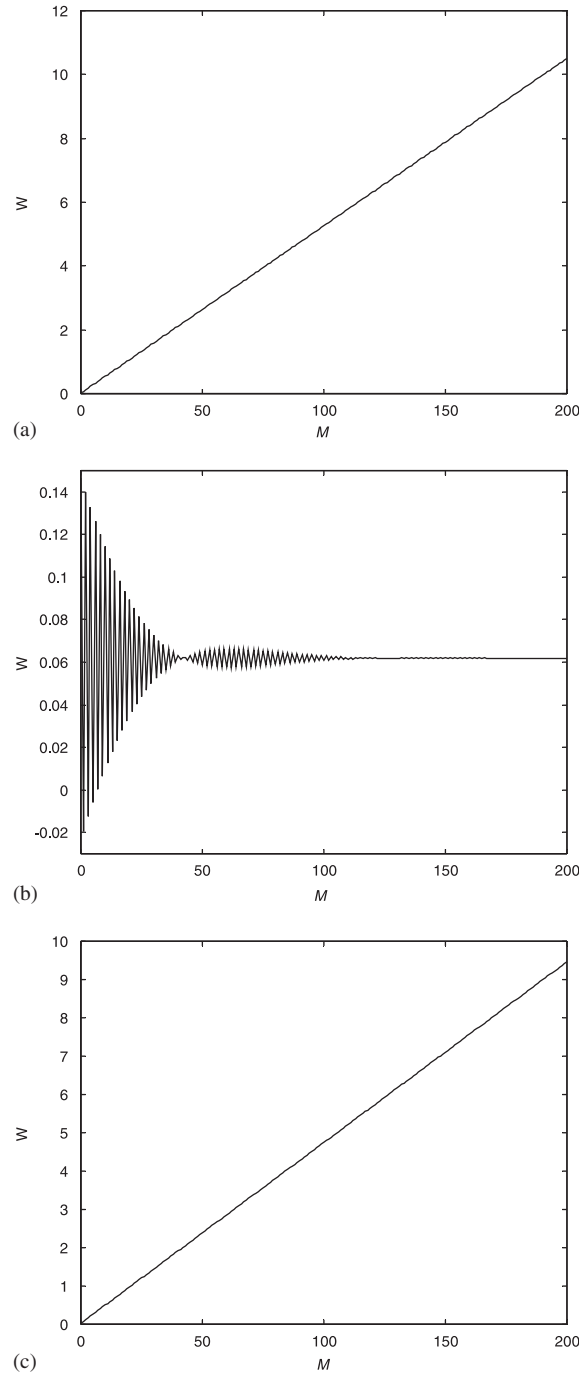


Fig. 8. Evolution of the amplitude of transverse displacement at the free end: (a) at the resonant frequency of the third mode (3409 Hz); (b) at an off-resonant frequency between the third and the fourth modes (4400 Hz); and (c) at the resonant frequency of the fourth mode (5376 Hz).

synchronization does not hold; hence the response shows fluctuation and converges to a final steady state with small amplitude.

An interesting question is how the initial waves evolve to the final response when the input energy is finite, e.g., the excitation is an impulse force. It is expected that final steady state with large but finite amplitude is achieved at resonance. However, this needs to be justified by further wave evolution analysis. The situation would become more complicated when damping is presented. These would be topics of a subsequent study.

The waves in the degenerate case can be regarded as special cases of Eqs. (48a) and (48b) where

$$\begin{pmatrix} m_{22} & -m_{12} \\ -m_{21} & m_{11} \end{pmatrix} = \begin{pmatrix} 1 & 0 \\ 0 & 1 \end{pmatrix} \text{ and } \begin{pmatrix} n_{22} & -n_{12} \\ -n_{21} & n_{11} \end{pmatrix} = \begin{pmatrix} 1 & 0 \\ 0 & 1 \end{pmatrix}.$$

Thus, the wave-train closure principle holds for realistic waves. In general, it could be concluded that the principle does not describe the realistic formulation process of a standing wave. It provides a convenient way to obtain vibration modes (resonant frequencies and mode shapes) from the point of view of wave propagation though.

5. Conclusions

In an attempt to justify the wave-mode duality and to elaborate on the physical understanding of the wave-train closure principle at resonance, forced beam vibration is simulated by a wave evolution approach. The beam is excited by external swept sinusoidal force at a location along the beam span. The expression of steady-state response is obtained by tracing the process of wave evolution starting from initial response. Since wave reflection at the boundaries of the beam can be classified as superposition and degenerate states, wave evolutions in these two states are traced separately. The condition of resonance is then derived from the expression of steady-state response, from which natural frequencies and mode shapes of vibration modes of a beam can be calculated. A simply supported beam and a cantilever beam are used as examples of the degenerate state and the superposition state, respectively, to justify the wave-mode duality at resonance. In the former case, analytical results are available, while in the latter case, numerical results are presented along with experimental measurements.

The wave-train closure principle is also examined. For both the superposition and the degenerate states, it is shown that the frequency equations obtained by using the wave-train closure principle are identical to those derived from the present wave evolution results. However, further examination shows that the principle does not describe the realistic process of the formulation of vibration modes in general. The waves described in the wave-train closure principle are generally not physical but “virtual” waves that represent final steady-state waves, which can only be asymptotically approached in reality. The principle can thus be used as a convenient technique to obtain vibration modes from the point of view of wave propagation.

Acknowledgments

Funding support given by the Research Grants Council of the Government of the HKSAR under Project Nos. PolyU5119/98E, PolyU5154/99E, PolyU5148/00E, PolyU5161/00E and PolyU1/02C are gratefully acknowledged.

Appendix

A list of wave reflection matrices for various boundary conditions as given by Wang and So [23]. K_B and T_B are translational and torsional spring constants of the elastic boundary supports, respectively. At the right boundary, $K_B = K_R$ and $T_B = T_R$, while at the left boundary, $K_B = K_L$ and $T_B = T_L$, where the subscripts ‘R’ and ‘L’ represent “right” and “left”, respectively.

	Elastically supported (Superposed at frequencies other than ω_{spe})	Elastically supported (Degenerate at ω_{spe})	Simply supported	Sliding
$[+R]$	$\begin{pmatrix} [(r_a + 1)K_B - ik_a KGA] & [(r_b + 1)K_B - ik_b KGA] \\ -r_a(k_a^2 EI - ik_a T_B) & -r_b(k_b^2 EI - ik_b T_B) \end{pmatrix}$	$\begin{pmatrix} [(r_a + 1)K_B - ik_a KGA] & 0 \\ 0 & [(r_b + 1)K_B - ik_b KGA] \end{pmatrix}$	$\begin{pmatrix} (r_a + 1) & 0 \\ 0 & (r_b + 1) \end{pmatrix}$	$\begin{pmatrix} ik_a r_a & 0 \\ 0 & ik_b r_b \end{pmatrix}$
$[-R] = [+R]^*$	$\begin{pmatrix} [(r_a + 1)K_B + ik_a KGA] & [(r_b + 1)K_B + ik_b KGA] \\ -r_a(k_a^2 EI + ik_a T_B) & -r_b(k_b^2 EI + ik_b T_B) \end{pmatrix}$	$\begin{pmatrix} [(r_a + 1)K_B + ik_a KGA] & 0 \\ 0 & [(r_b + 1)K_B + ik_b KGA] \end{pmatrix}$	$\begin{pmatrix} (r_a + 1) & 0 \\ 0 & (r_b + 1) \end{pmatrix}$	$\begin{pmatrix} -ik_a r_a & 0 \\ 0 & -ik_b r_b \end{pmatrix}$
Right-side boundary R_R	$-\{[-R]\}^{-1} [+R]$	$\begin{pmatrix} -\frac{[(r_a + 1)K_B - ik_a KGA]}{[(r_a + 1)K_B + ik_a KGA]} & 0 \\ 0 & -\frac{[(r_b + 1)K_B - ik_b KGA]}{[(r_b + 1)K_B + ik_b KGA]} \end{pmatrix} = \begin{pmatrix} -e^{-i\theta^{in}} & 0 \\ 0 & -e^{-i\theta^{out}} \end{pmatrix}$	$-\mathbf{I}$	\mathbf{I}
Left-side boundary R_L	$-\{[+R]\}^{-1} [-R]$	$\begin{pmatrix} -\frac{[(r_a + 1)K_B + ik_a KGA]}{[(r_a + 1)K_B - ik_a KGA]} & 0 \\ 0 & -\frac{[(r_b + 1)K_B + ik_b KGA]}{[(r_b + 1)K_B - ik_b KGA]} \end{pmatrix} = \begin{pmatrix} -e^{i\theta^{in}} & 0 \\ 0 & -e^{i\theta^{out}} \end{pmatrix}$	$-\mathbf{I}$	\mathbf{I}

References

- [1] R.H. Lyon, R.G. DeJong, *Theory and Application of Statistical Energy Analysis*, second ed., Butterworth-Heinemann, USA, 1995.
- [2] F.J. Fahy, Statistical energy analysis: a critical overview, *Philosophical Transactions of the Royal Society of London, Series A: Physical Sciences and Engineering* 346 (1994) 431–447.
- [3] O.M. Bouthier, R.J. Bernhard, Simple models of energy flow in vibrating membranes, *Journal of Sound and Vibration* 182 (1995) 129–147.
- [4] O.M. Bouthier, R.J. Bernhard, Simple models of energetics of transversely vibrating plates, *Journal of Sound and Vibration* 182 (1995) 149–166.
- [5] Y. Lase, M.N. Ichchou, L. Jezequel, Energy flow analysis of bars and beams: theoretical formulations, *Journal of Sound and Vibration* 192 (1996) 281–305.
- [6] R.M. Grice, R.J. Pinnington, A method for the vibration analysis of built-up structures, part I: introduction and analytical analysis of the plate-stiffened beam, *Journal of Sound and Vibration* 230 (2000) 825–849.
- [7] Y.C. Tan, M.P. Castanier, C. Pierre, Approximation of power flow between two coupled beams using statistical energy methods, *ASME Journal of Vibrations and Acoustics* 123 (2001) 510–523.
- [8] R.S. Langley, V. Cotoni, Response variance prediction in the statistical energy analysis of built-up systems, *Journal of the Acoustical Society of America* 115 (2004) 706–718.
- [9] M.P. Norton, *Fundamentals of Noise and Vibration Analysis for Engineers*, Cambridge University Press, Cambridge, 1989.
- [10] K.T. Chan, X.Q. Wang, R.M.C. So, S.R. Reid, Superposed standing waves in a Timoshenko beam, *Proceedings of the Royal Society of London, Series A* 458 (2002) 83–108.
- [11] S. Gopalakrishnan, J.F. Doyle, Spectral super-elements for wave propagation in structures with local non-uniformities, *Computational Methods in Applied Mechanics and Engineering* 121 (1995) 77–90.
- [12] R.S. Langley, P. Bremner, A hybrid method for the vibration analysis of complex structural-acoustic systems, *Journal of the Acoustical Society of America* 105 (1999) 1657–1671.
- [13] R.M. Grice, R.J. Pinnington, A method for the vibration analysis of built-up structures, part II: analysis of the plate-stiffened beam using a combination of finite element analysis and analytical impedances, *Journal of Sound and Vibration* 230 (2000) 851–875.
- [14] B.R. Mace, P.J. Shorter, Energy flow models from finite element analysis, *Journal of Sound and Vibration* 233 (2000) 369–389.
- [15] C. Mei, B.R. Mace, R.W. Jones, Hybrid wave/mode active vibration control, *Journal of Sound and Vibration* 247 (2001) 765–784.
- [16] D.R. Mahapatra, S. Gopalakrishnan, A spectral finite element for analysis of wave propagation in uniform composite tubes, *Journal of Sound and Vibration* 268 (2003) 429–463.
- [17] M. Ostoja-Starzewski, A. Woods, Spectral finite elements for vibrating rods and beams with random field properties, *Journal of Sound and Vibration* 268 (2003) 779–797.
- [18] J.B. Casimir, T. Vinh, C. Duforet, Dynamic behavior of structures in large frequency range by continuous element methods, *Journal of Sound and Vibration* 267 (2003) 1085–1106.
- [19] F. Birgersson, S. Finnveden, G. Robert, Modeling turbulence-induced vibration of pipes with a spectral finite element method, *Journal of Sound and Vibration* 278 (2004) 749–772.
- [20] R.S. Langley, Some perspectives on wave-mode duality in SEA, in: F.J. Fahy, W.G. Price, (Eds.), *Proceedings of the IUTAM Symposium on Statistical Energy Analysis*, Southampton, UK, 8–11 July 1997, pp. 1–12.
- [21] L.Q. Chen, Analysis of axial vibration of uniform rods by traveling wave method, *Mechanics and Practice* 18 (1996) 63–64 (in Chinese).
- [22] L. Cremer, M. Heckl, E.E. Ungar, *Structure-borne Sound*, second ed., Springer-Verlag, Berlin, Heidelberg, 1988.
- [23] X.Q. Wang, R.M.C. So, Various standing waves in a Timoshenko beam, *Journal of Sound and Vibration* 280 (2005) 311–328.
- [24] K.T. Chan, Entanglement of standing waves in a Timoshenko beam, *Proceedings of the Royal Society of London Series A*, under review (Paper No. PA20026).
- [25] D.J. Mead, Wave propagation in Timoshenko beams, *Strojnický Casopis* 36 (1985) 556–584.
- [26] X.Q. Wang, Free Vibration of Timoshenko Beam Partially Loaded with Distributed Mass, Ph.D. Thesis, The Hong Kong Polytechnic University, 1998.